Interconversion of W and Greenberger-Horne-Zeilinger states for Ising-coupled qubits with transverse global control

Vladimir M. Stojanović and Julian K. Nauth
Institut für Angewandte Physik, Technical University of Darmstadt, D-64289 Darmstadt, Germany
(Dated: December 1, 2022)

Interconversions of W and Greenberger-Horne-Zeilinger states in various physical systems are lately attracting considerable attention. We address this problem in the fairly general physical setting of qubit arrays with long-ranged (all-to-all) Ising-type qubit-qubit interaction, which are simultaneously acted upon by transverse Zeeman-type global control fields. Motivated in part by a recent Lie-algebraic result that implies state-to-state controllability of such a system for an arbitrary pair of states that are invariant with respect to qubit permutations, we present a detailed investigation of the state-interconversion problem in the three-qubit case. The envisioned interconversion protocol has the form of a pulse sequence that consists of two instantaneous (delta-shaped) control pulses, each of them corresponding to a global qubit rotation, and an Ising-interaction pulse of finite duration between them. Its construction relies heavily on the use of the (four-dimensional) permutation-invariant subspace (symmetric sector) of the three-qubit Hilbert space. In order to demonstrate the viability of the proposed state-interconversion scheme, we provide a detailed analysis of the robustness of the underlying pulse sequence to systematic errors, i.e. deviations from the optimal values of its five characteristic parameters.

I. INTRODUCTION

Regardless of their concrete physical realization, maximally-entangled multiqubit states are of utmost importance for quantum-information processing (QIP) [1]. Two prominent classes of such states, which cannot be transformed into each other through local operations and classical communication [2], are W [3] and Greenberger-Horne-Zeilinger (GHZ) [4] states. In particular, in the three-qubit case W and GHZ are the only two subclasses of states with genuine tripartite entanglement [5]. Both classes have proven useful in diverse QIP contexts [6–10], which was the primary motivation behind a large number of proposals for the efficient preparation of W [11–21] and GHZ states [12, 22–30] in various physical systems.

In view of the completely different characters of entanglement in W and GHZ states [3, 31], the interconversion between those states in different physical platforms represents an interesting, increasingly relevant problem of quantum-state engineering. The earliest attempt in the context of such an interconversion pertained to a photonic system [32]. This initial study, which was probabilistic in nature, was followed by another photon-related work [33] and an investigation of such interconversions in a spin system [34]. In the realm of atomic systems, irreversible conversions of W- into GHZ states were first proposed [35, 36]. More recently, the deterministic interconversion between the two states in a system of three Rydberg-atom-based qubits [37, 38] subject to four external laser pulses was extensively studied [39–42].

In this paper, the interconversion of W and GHZ states problem is addressed for an array of qubits coupled through Ising-type (ZZ) interaction, being also subject to two Zeeman-like global control fields in the transverse (x- and y) directions. The Ising-type coupling between qubits is of practical importance as it enables the realization of the controlled-Z gate (also known as the controlled phase-shift gate [43]). Namely, the Ising-coupling gate and controlled-Z are related by single-qubit z rotations and a global phase shift [43]. At the same time, the controlled-Z gate differs from controlled-NOT (CNOT) only by two Hadamard gates applied to the target qubit of the CNOT gate [1].

It is worthwhile pointing out that, generally speaking, global-control schemes for qubit arrays constitute a promising pathway towards scalable QC. Apart from obviating the need for local qubit addressing, which in some physical platforms for QC is unfeasible, another well-known advantage of such schemes stems from the fact that a continuous-wave global field can efficiently decouple qubits from the background noise [44].

The motivation behind the present work is twofold. Firstly, a qubit array with long-range Ising-type qubit-qubit interactions can be realized in various physical platforms for QC, from nuclear-magnetic-resonance (NMR) systems [45–47] to ensembles of neutral atoms in Rydberg states [37]; therefore, an efficient solution of the W-to-GHZ state-conversion problem may facilitate the realization of various QIP protocols in those systems. Secondly, a recent result in the realm of Lie-algebraic controllability implies that such an array of Ising-coupled qubits, which is subject to global control fields in the two transverse directions, is indeed state-to-state controllable provided that the two relevant (initial and final) states are invariant under an arbitrary permutation of qubits [48]; moreover, it is important to note that both W states and their GHZ counterparts are permutationally invariant for an arbitrary number of qubits.

While the aforementioned Lie-algebraic result [48] guarantees the existence of a quantum-control protocol for converting a W state into its GHZ counterpart for Ising-coupled qubits with global transverse control, a solution of the last problem for a three-qubit system is presented in this paper. The envisioned state-conversion

protocol is based on an NMR-type pulse sequence that consists of two instantaneous (delta-shaped) global control pulses and an Ising-interaction pulse of finite duration between them. The construction of this pulse sequence, as well as its robustness against errors in the relevant parameters (e.g. small variations of the duration of Ising-interaction pulses and global-rotation angles corresponding to the transverse control fields), are discussed in detail in what follows. It is worthwhile mentioning that pulse sequences of this kind have as yet been utilized in multiple physical contexts of interest for QIP [43, 49–52]. For example, they were proposed by one of us and collaborators for applications in measurement-based quantum computing [53], more precisely for preserving cluster states [54], as well as for dynamically generating code words of various quantum error-correction codes [55].

The remainder of the present paper is organized as follows. In Sec. II, the system under consideration and the state-conversion problem to be addressed in the following are introduced, along with the notation to be used throughout the paper. Section III is devoted to the symmetry-related aspects of the problem at hand, more precisely its invariance under an arbitrary permutation of qubits and the ensuing concept of the symmetric sector of the three-qubit Hilbert space. In addition, one familiar (symmetry-adapted) basis of the latter subspace is introduced. In Sec. IV the construction of an NMR-type pulse sequence, which represents one solution of the state-conversion problem in the three-qubit case, is discussed in detail. The principal results for the idealized pulse sequence behind the W-to-GHZ state conversion, as well as its robustness to errors in its characteristic parameters, are presented in Sec. V Finally, the paper is summarized – along with underscoring its main conclusions and possible generalizations – in Sec. VI.

II. SYSTEM AND W-TO-GHZ CONVERSION PROBLEM

The system under consideration is a qubit array with long-range Ising-type coupling with strength J, subject to global Zeeman-type control fields $h_x(t)$ and $h_y(t)$ in the x- and y directions, respectively. The total Hamiltonian of the system $H(t) = H_{ZZ} + H_C(t)$ consists of the drift (Ising-interaction) part H_{ZZ} and the global-control part $H_C(t)$. It can succinctly be written as

$$H(t) = H_{ZZ} + h_x(t)\mathcal{X} + h_y(t)\mathcal{Y} \,. \tag{1}$$

Here H_{ZZ}, $\mathcal{X}$, and $\mathcal{Y}$ are given by

$$H_{ZZ} \;=\; J \sum_{1\leq n<n'\leq N} Z_n Z_{n'} \,, \tag{2}$$

$$\mathcal{X} \;=\; \sum_{n=1}^{N} X_n \quad , \quad \mathcal{Y} = \sum_{n=1}^{N} Y_n \,, \tag{3}$$

where X_n, Y_n, and Z_n are the Pauli operators of qubit n ($n = 1, \ldots, N$):

$$\begin{aligned} X_n &= \mathbb{1}\otimes\ldots\otimes\mathbb{1}\otimes\underbrace{X}_{n}\otimes\mathbb{1}\otimes\ldots\otimes\mathbb{1}\,, \\ Y_n &= \mathbb{1}\otimes\ldots\otimes\mathbb{1}\otimes\underbrace{Y}_{n}\otimes\mathbb{1}\otimes\ldots\otimes\mathbb{1}\,, \\ Z_n &= \mathbb{1}\otimes\ldots\otimes\mathbb{1}\otimes\underbrace{Z}_{n}\otimes\mathbb{1}\otimes\ldots\otimes\mathbb{1}\,. \end{aligned} \tag{4}$$

It is pertinent to comment on the controllability [56] aspects of systems described by the Hamiltonian of Eq. (1). In this context, it is useful to first point out that for complete operator controllability (implying the ability to realize an arbitrary unitary transformation on the Hilbert space of the underlying system, i.e. universal quantum computation) of a qubit array with Ising-type interaction it is required to have two mutually noncommuting (local) controls acting on each qubit in the array [57]. In fact, it is only for qubit arrays with Heisenberg-type interaction (isotropic, XXZ-, or XYZ-type) that a significantly reduced degree of control – namely, two noncommuting controls acting on a single qubit in the array – guarantees complete controllability [57, 58]. Thus, a system of N qubits that are coupled through Ising-type interaction and subject to global Zeeman-like control fields in the x- and y directions [cf. Eqs. (1)-(3) above], is in general not completely operator controllable; in other words, its dynamical Lie algebra [56] $\mathcal{L}_d = \mathrm{span}\{H_{ZZ}, \mathcal{X}, \mathcal{Y}\}$ is not isomorphic with $u(2^N)$ or $su(2^N)$, but with their proper Lie subalgebra.

Despite the lack of complete controllability, it has recently been demonstrated that a system described by the Hamiltonian in Eq. (1), which is manifestly symmetric with respect to an arbitrary permutation of qubits (i.e. spin-1/2 subsystems), is controllable provided one restricts oneself to unitary evolutions that preserve this permutation invariance [48]. An immediate implication of this last result is that such a system is state-to-state controllable for any pair of states that are themselves invariant with respect to qubit permutations. This is equivalent to the statement that the time-dependence of control fields $h_x(t)$ and $h_y(t)$ in Eq. (1) can be found such that one can reach any permutationally invariant final state in a finite time starting from an arbitrary permutationally invariant state at $t = 0$. As usual for Lie-algebraic controllability theorems [56], which have the character of existence theorems, the actual time-dependence of these control fields that enables a controlled dynamical evolution of the system from a given initial- to a desired final state has to be determined in each particular case [59].

In what follows, we design protocols for the deterministic interconversion of W and GHZ state in a three-qubit system ($N = 3$). The general expressions of Eqs. (2) and

(3) in that case reduce to

$$\begin{aligned} H_{ZZ} &= J(Z_1Z_2 + Z_2Z_3 + Z_1Z_3)\,, \\ \mathcal{X} &= X_1 + X_2 + X_3\,, \\ \mathcal{Y} &= Y_1 + Y_2 + Y_3\,, \end{aligned} \tag{5}$$

where – in line with the general definition of X_n, Y_n, Z_n [cf. Eq. (4)] – the operators $X_1, X_2 \ldots, Z_3$ are represented in the standard computational basis by eight-dimensional matrices.

Because W and GHZ states both have the property of being permutation-invariant (for an arbitrary number of qubits), our treatment of the state-conversion problem for a three-qubit system will rely heavily on this last property of the initial and final states. More precisely, in the following a protocol is sought after that allows the conversion of an initial W state into a GHZ state; the inverse state-conversion process – converting an initial GHZ state into its W-state counterpart – is analyzed in an analogous fashion. In other words, the state $|\psi(t)\rangle$ of our three-qubit system should satisfy the conditions

$$\begin{aligned} |\psi(t=0)\rangle &= |W_3\rangle = \frac{1}{\sqrt{3}}\left(|100\rangle + |010\rangle + |001\rangle\right)\,, \\ |\psi(t=T)\rangle &= |\mathrm{GHZ}_3(\varphi)\rangle = \frac{1}{\sqrt{2}}\left(|000\rangle + e^{i\varphi}|111\rangle\right)\,, \end{aligned} \tag{6}$$

where $\varphi \in [0, 2\pi)$ and T is the state-conversion time.

The W-to-GHZ state conversion will be achieved here using an NMR-type pulse sequence. Such sequences consist of a certain number of instantaneous (delta-shaped) control pulses and Ising-interaction pulses in between the control pulses. In the following, we set $\hbar = 1$, hence all the relevant timescales in the problem at hand will be expressed in units of the inverse Ising-coupling strength J^{-1}.

III. SYMMETRIC SECTOR AND ITS BASIS

In what follows, we describe the problem under consideration by exploiting its permutation-symmetric character. To this end, we first introduce the concept of the symmetric sector of the three-qubit Hilbert space and define one specific basis of this sector that facilitates the solution of the state-conversion problem at hand.

In a variety of problems in quantum control and quantum-state engineering it is beneficial to consider pure states that are invariant with respect to permutations of qubits [60–65]. In this context, we can distinguish situations where the relevant states are those invariant under an arbitrary permutation – i.e. the full symmetric group S_n, where n is the number of qubits [64] – and those where the relevant states are invariant with respect to specific nontrivial subgroups of S_n [65].

In the state-conversion problem at hand, we focus on the subset of all the unitaries on the Hilbert space $\mathcal{H} \equiv (\mathbb{C}^2)^{\otimes 3}$ of the three-qubit system under consideration that are invariant under an arbitrary qubit permutation, i.e. the permutation group S_3. The relevant Lie subgroup of $U(8)$ is denoted by $U^{\mathrm{S}_3}(8)$ and has dimension equal to 20 [48]. Its corresponding Lie algebra $u^{\mathrm{S}_3}(8)$ is spanned by the operators $i\Pi(\sigma_1 \otimes \sigma_2 \otimes \sigma_3)$, where $\Pi = (3!)^{-1}\sum_{P\in S_3} P$ and σ_n $(n = 1, 2, 3)$ is either the single-qubit identity operator $\mathbb{1}_2$ or one of the Pauli operators X, Y, Z.

Under the action of the Lie algebra $u^{\mathrm{S}_3}(8)$ the 8-dimensional Hilbert space $\mathcal{H}$ splits into three invariant subspaces that correspond to irreducible representations of $su(2)$. Two of those subspaces have dimension 2, while the third one has dimension 4 and is uniquely determined. The latter is usually referred to as the *symmetric sector* [61], because it comprises the states that do not change under an arbitrary permutation of qubits. One orthonormal, symmetry-adapted basis of the symmetric sector is given by the states $\{|\zeta_a\rangle|\, a = 0, \ldots, 3\}$, where

$$\begin{aligned} &|\zeta_0\rangle = |000\rangle\,, \quad |\zeta_1\rangle = \frac{1}{\sqrt{3}}\left(|100\rangle + |010\rangle + |001\rangle\right)\,, \\ &|\zeta_2\rangle = \frac{1}{\sqrt{3}}\left(|110\rangle + |101\rangle + |011\rangle\right)\,, \quad |\zeta_3\rangle = |111\rangle\,, \end{aligned} \tag{7}$$

and the subscript a in $|\zeta_a\rangle$ coincides with the Hamming weight of the corresponding bit string (i.e. the number of occurrences of 1 in that bit string) [66]. It is obvious that $|\zeta_1\rangle \equiv |W_3\rangle$ is the W state itself, while $|\zeta_2\rangle$ corresponds to the two-excitation Dicke state.

In the following, we consider the state-conversion problem within the symmetric sector using the basis defined in Eq. (7). To begin with, we map the four basis states onto column vectors according to

$$\begin{aligned} |\zeta_0\rangle &\mapsto \begin{pmatrix} 1 \\ 0 \\ 0 \\ 0 \end{pmatrix}, \quad |\zeta_1\rangle \mapsto \begin{pmatrix} 0 \\ 1 \\ 0 \\ 0 \end{pmatrix}, \\ |\zeta_2\rangle &\mapsto \begin{pmatrix} 0 \\ 0 \\ 1 \\ 0 \end{pmatrix}, \quad |\zeta_3\rangle \mapsto \begin{pmatrix} 0 \\ 0 \\ 0 \\ 1 \end{pmatrix}. \end{aligned} \tag{8}$$

We also can straightforwardly represent the initial and target states of our envisioned state conversion [cf. Eq. (6)] in this same basis. While $|\zeta_1\rangle \equiv |W_3\rangle$, the GHZ state is given by

$$|\mathrm{GHZ}_3(\varphi)\rangle \mapsto \frac{1}{\sqrt{2}}\begin{pmatrix} 1 \\ 0 \\ 0 \\ e^{i\varphi} \end{pmatrix}. \tag{9}$$

For the sake of completeness, it is worthwhile mentioning that a generalized Schmidt decomposition allowed a classification of pure three-qubit states [67]. More specifically yet, in Ref. [67] it was demonstrated that five independent nonzero real parameters are needed to describe

the entire three-qubit state space under local operations; in other words, a generic pure three-qubit state is equivalent under local unitary transformations to a canonical state described by these five parameters. It was shown that there exist, in fact, three inequivalent sets of five local basis product states, where each of these three sets contains the states $|000\rangle$, $|100\rangle$, and $|111\rangle$. One of those sets, given by $\{|000\rangle, |001\rangle, |010\rangle, |100\rangle, |111\rangle\}$, is symmetric with respect to permutations of qubits (parties) and yields three-qubit W and GHZ states as linear combinations of its elements. It is also worthwhile pointing out that an experimental scheme for creating a generic pure three-qubit state in NMR – in line with the classification in Ref. [67] – was proposed in the past [12].

IV. W-TO-GHZ STATE CONVERSION USING A PULSE SEQUENCE

We aim to find a solution of the W-to-GHZ state conversion problem [cf. Eq. (6)] for an arbitrary value of φ. As indicated above, the two states of interest are invariant with respect to an arbitrary permutation of qubits. Thus, the problem can be reduced to the symmetric sector and its basis given in Eq. (7) above.

In the following, we first describe the layout of the envisioned pulse sequence for implementing W-to-GHZ state conversion (Sec. IV A), followed by the derivation of the time-evolution operators corresponding to different parts of this pulse sequence (Sec. IV B).

A. Form of the pulse sequence

We seek a solution to the W-to-GHZ state conversion problem in the form of an NMR-type pulse sequence that consists of two instantaneous control pulses – at times $t = 0$ and $t = T$ (i.e. with a time delay T between them) – and an Ising-interaction pulse with duration T between these control pulses (for a pictorial illustration, see Fig. 1 below). The corresponding transverse (global) control field $\boldsymbol{h}(t) \equiv [h_x(t), h_y(t), 0]^{\mathrm{T}}$ can be written as

$$\boldsymbol{h}(t) = \boldsymbol{\alpha}_1 \delta(t) + \boldsymbol{\alpha}_2 \delta(t - T)\,, \tag{10}$$

where the two delta functions capture the instantaneous character of the two control pulses and the vectors $\boldsymbol{\alpha}_1$ and $\boldsymbol{\alpha}_2$ point in arbitrary directions in the x-y plane; the corresponding directions are specified by their polar angles ϕ_1 and ϕ_2, respectively, where $\phi_1, \phi_2 \in [0, 2\pi)$.

Before embarking on the derivation of the respective time-evolution operators that correspond to different parts of the envisioned pulse sequence (cf. Fig. 1), it is pertinent to comment on the feasibility of realizing such pulse sequences in various physical platforms for QC. Firstly, the assumption of instantaneous control pulses is well justified whenever the control fields used are much stronger than the coupling between qubits; this requirement is, for example, satisfied for typical control magnetic fields used in the NMR realm [45], as well as for typical control fields in superconducting-qubit- [50] and neutral-atom systems [37]. Secondly, the fact that the envisioned pulse sequence entails single-qubit rotations about two different axes in the x-y plane is feasible in practice. Namely, modification of the rotation axis of a single-qubit drive represents a rather straightforward operation in currently used platforms for QC, such as neutral atoms [68], superconducting qubits [69], and trapped ions [70]; such an operation does not involve much of an additional experimental complexity or overhead.

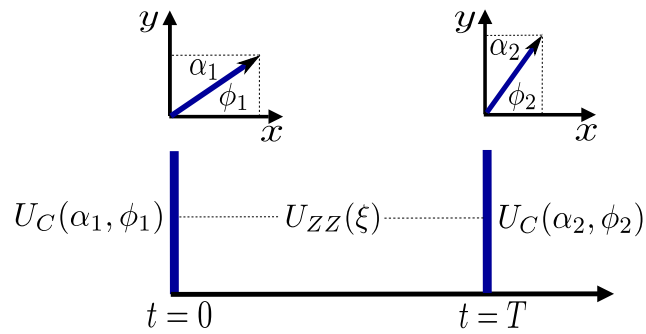

FIG. 1: (Color online)Pictorial illustration of the pulse sequence for realizing the W-to-GHZ state conversion, which consists of two instantaneous control pulses and an Ising-interaction pulse of finite duration T between them. The first (second) control pulse is characterized by a vector in the x-y plane, with the magnitude α_1 (α_2) and polar angle ϕ_1 (ϕ_2). Here $U_C(\alpha_1, \phi_1)$ and $U_C(\alpha_2, \phi_2)$ are the time-evolution operators corresponding to the control pulses at $t = 0$ and $t = T$, respectively; $U_{ZZ}(\xi)$ corresponds to the interaction pulse, with $\xi \equiv JT$ being its dimensionless duration.

It is important to stress that the global character of single-qubit rotations in the envisioned pulse sequence is, in fact, a necessity in many QC platforms under current investigation. An example is furnished by a typical setup for neutral-atom QC, both in cases where the role of two logical states of a qubit is played by two hyperfine states (gg qubits) and in cases where a ground state and a high-lying Rydberg state play this role (gr qubits). In such neutral-atom systems one typically makes use of a global microwave field – which in the case of gg qubits has the physical nature of magnetic dipole coupling – to carry out a rotation about an arbitrary axis in the $x - y$ plane on every qubit [71]; at the same time, the rotation axis can be chosen by modifying the phase of the microwave field. Importantly, this rotation gate ought to be global in nature because the distance between qubits in such systems (typically a few micrometers) is far smaller than the wavelength of the microwave field ($1\,\mathrm{mm} \lesssim \lambda \lesssim 1\,\mathrm{m}$); as a result, each qubit undergoes the same rotation.

While here we aim for an analog implementation of the envisioned pulse sequence, it should be stressed that such a pulse sequence is also amenable to an efficient digital realization in various QC platforms. For example, in the neutral-atom platform a rotation over an arbitrary axis in

the $x-y$ plane – represented by a two-parameter (single-qubit) gate U_{xy} – constitutes the essential single-qubit operation [37]; this gate allows one to realize an arbitrary single-qubit rotation and – by extension – any single-qubit operation (e.g. the Hadamard gate). The situation is even more favorable in the case of typical trapped-ion QC setups [72], where the native get set includes not only $x-y$ rotations but also a ZZ two-qubit gate (therefore, the Ising-interaction pulse in the problem at hand could be implemented in that platform through a sequence of three pairwise ZZ gates); in addition, the trapped-ion platform has the advantage of allowing perfect (all-to-all) connectivity between individual qubits.

As substantiated above, global-control- and interaction pulses required for the realization of the envisaged state interconversion represent the basic gate operations in systems with Ising-type qubit-qubit coupling [43, 73]. For completeness, it is interesting to note that those types of pulses are formally equivalent with the two unitary operations utilized in the generalized form of the quantum approximate optimization algorithm (QAOA) [74]. More precisely, the Ising-interaction pulse corresponds to the cost-Hamiltonian-based unitary operator, as the Ising model encodes the cost function of a typical combinatorial-optimization problem (e.g. Max-Cut). At the same time, our global control pulses have the same form as the mixing-Hamiltonian unitary in QAOA under the assumption that the latter is generalized so as to involve not only the Pauli-X but also Y operators. The corresponding rotation angles should be the same for different qubits and only vary between different rounds, which is one of the already investigated modifications of the original QAOA algorithm.

B. Relevant time-evolution operators

In what follows, we present the derivation of the time-evolution operators describing the control- and Ising-interaction pulses enabling the W-to-GHZ state conversion in the three-qubit system under consideration.

Using the form of the Ising-interaction Hamiltonian [cf. Eq. (5)] in the chosen symmetry-adapted basis [cf. Eq. (8)],

$$H_{ZZ} \mapsto J \begin{pmatrix} 3 & 0 & 0 & 0 \\ 0 & -1 & 0 & 0 \\ 0 & 0 & -1 & 0 \\ 0 & 0 & 0 & 3 \end{pmatrix} , \tag{11}$$

it is straightforward to derive the time-evolution operator corresponding to the Ising interaction pulse (cf. Fig. 1). This time-evolution operator is given by

$$U_{ZZ}(\xi) = e^{-i\xi H_{ZZ}/J} \mapsto \begin{pmatrix} e^{-3i\xi} & 0 & 0 & 0 \\ 0 & e^{i\xi} & 0 & 0 \\ 0 & 0 & e^{i\xi} & 0 \\ 0 & 0 & 0 & e^{-3i\xi} \end{pmatrix} , \tag{12}$$

where $\xi \equiv JT$ is the dimensionless duration of the Ising-interaction pulse (i.e. the time delay between the two control pulses).

We now address the form of the time-evolution operator of one instantaneous (delta-shaped) control pulse [cf. Eq. (10)]. Even though the corresponding (time-dependent) control Hamiltonian involves the mutually noncommuting Pauli operators X_n and Y_n ($n = 1, 2, 3$), the time-dependence of the x- and y control fields is the same, which implies that this control Hamiltonian has the property of commuting with itself at different times (i.e. $[H_C(t), H_C(t')] = 0$). Consequently, its corresponding time-evolution operator is given by $\exp[-i \int_{t_i}^{t_f} H_C(t)dt]$ (where t_i and t_f are the initial and final evolution times, respectively), rather than requiring a time-ordered exponential (Dyson series). This operator is given by an exponential of a linear combination of the Pauli operators X_n and Y_n and can be evaluated using the well-known identity for single-qubit rotation operators

$$\exp[-i\theta(\hat{\mathbf{n}} \cdot \mathbf{X})] = \cos\theta \mathbb{1}_2 - i \sin\theta \, (\hat{\mathbf{n}} \cdot \mathbf{X}) , \tag{13}$$

where $\mathbf{X} \equiv (X, Y, Z)^{\mathrm{T}}$ is the vector of Pauli operators, and $\hat{\mathbf{n}}$ is an arbitrary unit vector. The left-hand-side of the last equation corresponds to the rotation through an angle of 2θ around the axis defined by the vector $\hat{\mathbf{n}}$, i.e. the rotation represented by the operator $R_{\hat{\mathbf{n}}}(2\theta)$.

By making use of the last identity, we obtain the time-evolution operators $U_C(\boldsymbol{\alpha})$ corresponding to individual control pulses; in the problem at hand $\boldsymbol{\alpha} = \boldsymbol{\alpha}_1$ for the first control pulse and $\boldsymbol{\alpha} = \boldsymbol{\alpha}_2$ for the second one. These time-evolution operators are of the form

$$U_C(\boldsymbol{\alpha}) = \prod_{n=1}^{3} (\cos\alpha \, \mathbb{1}_8 - i \sin\alpha \, \mathcal{A}_n) , \tag{14}$$

where $\mathcal{A}_n$ ($n = 1, 2, 3$) are auxiliary operators given by

$$\mathcal{A}_n = \frac{1}{\alpha} (\alpha_x X_n + \alpha_y Y_n) \tag{15}$$

and $\alpha \equiv \|\boldsymbol{\alpha}\| > 0$ denotes the norm of the vector $\boldsymbol{\alpha}$. By making use of the polar coordinates in the x-y plane, the operator $\mathcal{A}_n$ on qubit n can be recast in an exceedingly simple matrix form using

$$\frac{1}{\alpha} (\alpha_x X + \alpha_y Y) = \begin{pmatrix} 0 & e^{-i\phi} \\ e^{i\phi} & 0 \end{pmatrix} \tag{16}$$

for each qubit, where ϕ designates the polar angle corresponding to the vector $\boldsymbol{\alpha}$. By analogy with the general case represented by Eq. (13), an instantaneous control pulse in the system under consideration amounts to a global rotation through an angle of 2α around the axis whose direction is specified by the unit vector $\hat{\mathbf{n}} \equiv (\cos\phi, \sin\phi, 0)^{\mathrm{T}}$.

To obtain a more explicit form of $U_C(\boldsymbol{\alpha})$, we perform the multiplication in Eq. (14) and arrive at the expression

$$\begin{aligned} U_C(\boldsymbol{\alpha}) \; &= \; \cos^3\alpha \, \mathbb{1}_8 - i \sin\alpha \cos^2\alpha \, \mathcal{S}_1 \\ &- \; \sin^2\alpha \cos\alpha \, \mathcal{S}_2 + i \sin^3\alpha \, \mathcal{S}_3 , \end{aligned} \tag{17}$$

where $\mathcal{S}_1$, $\mathcal{S}_2$, and $\mathcal{S}_3$ are auxiliary operators given by

$$\begin{aligned} \mathcal{S}_1 &= \sum_{n=1}^{3} \mathcal{A}_n \,, \\ \mathcal{S}_2 &= \sum_{n<n'} \mathcal{A}_n \mathcal{A}_{n'} \,, \\ \mathcal{S}_3 &= \prod_{n=1}^{3} \mathcal{A}_n \,. \end{aligned} \tag{18}$$

When expressed in the basis of Eq. (8), these operators are represented by the 4×4 matrices

$$\begin{aligned} P_S \mathcal{S}_1 P_S^\dagger &= \begin{pmatrix} 0 & \sqrt{3}\, e^{-i\phi} & 0 & 0 \\ \sqrt{3}\, e^{i\phi} & 0 & 2e^{-i\phi} & 0 \\ 0 & 2e^{i\phi} & 0 & \sqrt{3}\, e^{-i\phi} \\ 0 & 0 & \sqrt{3}\, e^{i\phi} & 0 \end{pmatrix} , \\ P_S \mathcal{S}_2 P_S^\dagger &= \begin{pmatrix} 0 & 0 & \sqrt{3}\, e^{-2i\phi} & 0 \\ 0 & 2 & 0 & \sqrt{3}\, e^{-2i\phi} \\ \sqrt{3}\, e^{2i\phi} & 0 & 2 & 0 \\ 0 & \sqrt{3}\, e^{2i\phi} & 0 & 0 \end{pmatrix} , \\ P_S \mathcal{S}_3 P_S^\dagger &= \begin{pmatrix} 0 & 0 & 0 & e^{-3i\phi} \\ 0 & 0 & e^{-i\phi} & 0 \\ 0 & e^{i\phi} & 0 & 0 \\ e^{3i\phi} & 0 & 0 & 0 \end{pmatrix} , \end{aligned} \tag{19}$$

where P_S is the projector on the (four-dimensional) symmetric sector [cf. Eqs. (7) and (8)].

The time-evolution operator $U_C(\boldsymbol{\alpha}_1) \equiv U_C(\alpha_1, \phi_1)$ corresponding to the first ($t = 0$) control pulse and its counterpart $U_C(\boldsymbol{\alpha}_2) \equiv U_C(\alpha_2, \phi_2)$ that pertains to the second ($t = T$) pulse are straightforwardly obtained using Eqs. (17)-(19) [the cumbersome – but otherwise straightforward to derive – final expressions are not provided here]. By combining the final expressions for $U_C(\alpha_1, \phi_1)$ and $U_C(\alpha_2, \phi_2)$ with the previously derived expression for $U_{ZZ}(\xi)$ [cf. Eq. (12)], one recovers the time-evolution operator

$$\mathcal{U}(\xi, \boldsymbol{\alpha}_1, \boldsymbol{\alpha}_2) = U_C(\alpha_2, \phi_2)\, U_{ZZ}(\xi)\, U_C(\alpha_1, \phi_1) \tag{20}$$

that corresponds to the entire pulse sequence (for an illustration, see Fig. 1).

V. STATE-CONVERSION PROTOCOL: RESULTS AND DISCUSSION

In the following, we present and discuss the result for the state-conversion protocol based on the pulse sequence of Sec. IV. We first discuss the results obtained through numerical optimization of the GHZ-state fidelity corresponding to this pulse sequence (Sec. V A). We then consider the robustness of the state-conversion protocol to errors in its characteristic parameters (Sec. V B).

A. Optimization of the target-state fidelity

Aiming to convert the initial state $|W_3\rangle$ into $|\mathrm{GHZ}_3(\varphi)\rangle$ for an arbitrary value of φ, we maximize the central figure of merit in the problem at hand – the GHZ-state fidelity $\mathcal{F}_{\mathrm{GHZ}}(\varphi)$ – with respect to the parameters ξ, α_1, ϕ_1, α_2, and ϕ_2 characterizing the envisaged pulse sequence (cf. Sec. IV). This fidelity is given by

$$\mathcal{F}_{\mathrm{GHZ}}(\varphi) = |\langle \mathrm{GHZ}_3(\varphi)| \mathcal{U}(\xi, \boldsymbol{\alpha}_1, \boldsymbol{\alpha}_2) |W_3\rangle| \,, \tag{21}$$

i.e. by the module of the overlap of the target state $|\mathrm{GHZ}_3(\varphi)\rangle$ and the actual state $\mathcal{U}(\xi, \boldsymbol{\alpha}_1, \boldsymbol{\alpha}_2)|W_3\rangle$ obtained at the end of the pulse sequence [cf. Eq. (20)]. Given that the target GHZ state in the state-conversion problem at hand is parameterized by φ [cf. Eq. (6)], it is plausible to expect that the values (ξ_0,$\alpha_{1,0}$, $\phi_{1,0}$, $\alpha_{2,0}$, $\phi_{2,0}$) of these parameters that correspond to the maximum of $\mathcal{F}_{\mathrm{GHZ}}(\varphi)$ should also depend on φ.

We first carry out the optimization of the fidelity in Eq. (21) numerically for $\varphi = 0$ using the `minimize` routine from the `scipy.optimization` package [75] of the SciPy library. In this manner, we obtain the optimal values $\xi_0 = 0.3077$, $\alpha_{1,0} = \pi/4$, and $\alpha_{2,0} = 0.3077$ for the parameters ξ, α_1, and α_2, respectively. At the same time, for ϕ_1 and ϕ_2 we find three different branches of optimal values

$$(\phi_{1,0}, \phi_{2,0}) = \{(5\pi/6, \pi/3), (3\pi/2, \pi), (\pi/6, 5\pi/3)\} \,, \tag{22}$$

which correspond to three different choices for the directions of the global-rotation axes. As illustrated by Fig. 2, in all three cases the rotation axes corresponding to the control pulses are mutually perpendicular. Assuming that we choose $\phi_{1,0} = 5\pi/6$ (along with $\phi_{2,0} = \pi/3$) [cf. Eq. (22)], the first control pulse of the envisioned pulse sequence is equivalent to a global qubit rotation through an angle of $2\alpha_{1,0} = \pi/2$, around the axis specified by the unit vector $\hat{\mathbf{n}}_1 \equiv (-\sqrt{3}/2, 1/2, 0)^{\mathrm{T}}$.

The numerically obtained optimal values of ξ_0 and $\alpha_{2,0}$ can be made plausible in the following manner. By inserting the obtained values of $\alpha_{1,0}$, $\phi_{1,0}$, and $\phi_{2,0}$ – along with the observation that $\xi_0 = \alpha_{2,0}$ – into the general expression for $\mathcal{F}_{\mathrm{GHZ}}(\varphi)$ [cf. Eq. (21)], we obtain

$$\mathcal{F}_{\mathrm{GHZ}}(\varphi) = \frac{\sqrt{3}}{4} \sqrt{5 + 2\cos(4\xi_0) - 3\cos^2(4\xi_0)} \left|\cos(\frac{\varphi}{2})\right| \,. \tag{23}$$

Based on this last expression, $\mathcal{F}_{\mathrm{GHZ}}(\varphi) = 1$ if $\cos(4\xi_0) = 1/3$ and $\varphi = 0$. Therefore, the optimal values of ξ and α_2 are given by

$$\xi_0 = \alpha_{2,0} = \frac{1}{4} \arccos \frac{1}{3} \,, \tag{24}$$

which is equal to 0.3077 found numerically.

By choosing $\phi_{2,0} = \pi/3$ (along with $\phi_{1,0} = 5\pi/6$) [cf. Eq. (22)] the second control pulse of the envisioned pulse sequence amounts to a global qubit rotation through an

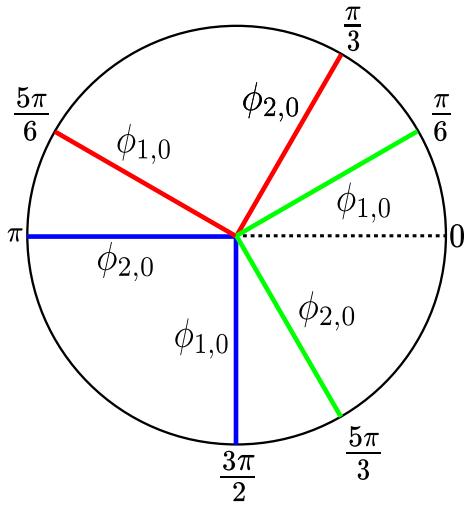

FIG. 2: (Color online)Pictorial illustration of the three branches of optimal values $\phi_{1,0}$ and $\phi_{2,0}$ of the angles that specify the directions of the global-rotation axes corresponding to the control pulses.

angle of $2\alpha_{2,0} = \arccos(1/3)/2$, around the axis specified by the unit vector $\hat{\mathbf{n}}_2 \equiv (1/2, \sqrt{3}/2, 0)^{\mathrm{T}}$.

Given that the envisaged pulse sequence entails two instantaneous control pulses, the total duration of the pulse sequence is effectively given by ξ – the (dimensionless) duration of the Ising-interaction pulse. Therefore, to verify that the obtained value ξ_0 of this last parameter indeed represents the minimal possible pulse-sequence duration that allows one to reach the GHZ-state fidelity close to unity, we performed the following numerical check. We reduced ξ to values below ξ_0 and tried to maximize $\mathcal{F}_{\mathrm{GHZ}}(\varphi = 0)$ with respect to the remaining four parameters. By so doing, we corroborated that $\xi_0 = \arccos(1/3)/4$ (i.e. $T_0 = 0.3077\ J^{-1}$ upon reinstating the dimensionful units) is indeed the sought-after minimal pulse-sequence duration that enables one to carry out the desired W-to-GHZ state conversion.

Having obtained the optimal values of the five pulse-sequence parameters for $\varphi = 0$, we performed numerical optimization of the GHZ-state fidelity for 100 nonzero values of φ in $[0, 2\pi)$. These calculations lead to two important conclusions. Firstly, the optimal values $\alpha_{1,0}, \alpha_{2,0}, \xi_0$ are completely independent of φ. Secondly, the optimal values of $\phi_{1,0}$ and $\phi_{2,0}$ depend linearly on φ. More specifically yet, the following linear dependencies are recovered from the obtained numerical results:

$$\begin{aligned} \phi_{1,0} &= \varphi/3 + 2\pi m/3 + 5\pi/6\,, \\ \phi_{2,0} &= \varphi/3 + 2\pi m/3 + \pi/3\,, \end{aligned} \tag{25}$$

where $m = 0, 1, 2$ enumerates different branches of optimal values.

From the form of the last equation it can be inferred why there are three branches of possible solutions for the optimal values of the parameters ϕ_1 and ϕ_2 [cf. Eq. (22)]. Namely, adding multiples of 2π to φ does not change the GHZ state itself [cf. Eq. (6)], while it yields additional possible values of $\phi_{1,0}$ and $\phi_{2,0}$ in $[0, 2\pi)$. More specifically yet, by adding 2π to the value $\varphi = 0$ (that yields $\phi_{1,0} = 5\pi/6$, $\phi_{2,0} = \pi/3$) one obtains $\phi_{1,0} = 3\pi/2$, $\phi_{2,0} = \pi$, while by adding 4π one finds $\phi_{1,0} = \pi/6$, $\phi_{2,0} = 5\pi/3$ (for an illustration, see Fig. 2).

For the sake of completeness, having considered W-to-GHZ state conversion it is worthwhile to briefly comment on the reversed state-conversion process, i.e. the one whereby an initial ($t = 0$) GHZ state is converted into a W state ($t = T$). The first instantaneous control pulse – acting on a GHZ state at $t = 0$ – is parameterized by α_2 and ϕ_2, while the second one (at $t = T$) is characterized by the parameters α_1 and ϕ_1. Our numerical optimization of the W-state fidelity – defined by analogy with Eq. (21) – leads to the conclusion that the optimal values of the parameters α_1, α_2, and ξ remain the same, while the three branches of solutions for $\phi_{1,0}$ and $\phi_{2,0}$ are in this case given by

$$(\phi_{1,0}, \phi_{2,0}) = \{(7\pi/6, 5\pi/3), (\pi/2, \pi), (11\pi/6, \pi/3)\}\,. \tag{26}$$

Finally, the counterpart of Eq. (25) in the case of GHZ-to-W state conversion reads as follows:

$$\begin{aligned} \phi_{1,0} &= -\varphi/3 + 2\pi m/3 + 7\pi/6\,, \\ \phi_{2,0} &= -\varphi/3 + 2\pi m/3 + 5\pi/3\,. \end{aligned} \tag{27}$$

B. Robustness of the state-conversion scheme to errors

Having obtained the parameter values that correspond to W-to-GHZ state conversion in Sec. V A, we now discuss the robustness of the envisaged state-conversion scheme to errors in those parameters. For definiteness, we mostly discuss this issue in the $\varphi = 0$ case; for a generic value of φ the discussion would be fairly similar.

In the NMR realm it is common to consider various imperfections in pulse-sequence realizations [45]. They typically amount to an error in the rotation axis (i.e. the direction of its corresponding unit vector $\hat{\mathbf{n}}$) and/or an error in the rotation angle. Therefore, the actual qubit rotation applied is not the ideal $R_{\hat{\mathbf{n}}}(2\theta) \equiv \exp[-i\theta(\hat{\mathbf{n}}\cdot\mathbf{X})]$ [cf. Eq. (13)], but is instead given by

$$\tilde{R}_{\hat{\mathbf{n}}}(2\theta) = \exp\left[-i\,\mathbf{f}(\theta, \hat{\mathbf{n}})\cdot\mathbf{X}\right]\,, \tag{28}$$

where $\mathbf{f}(\theta, \hat{\mathbf{n}})$ is a vector function that characterizes the systematic error [45]. For instance, $\mathbf{f}(\theta, \hat{\mathbf{n}}) = \theta(1 + \varepsilon_\theta)\hat{\mathbf{n}}$ describes under- and over-rotation errors (for negative- and positive values of ε_θ, respectively). At the same time, $\mathbf{f}(\theta, \hat{\mathbf{n}}) = \theta(n_x \cos\varepsilon_\phi + n_y \sin\varepsilon_\phi, n_y \cos\varepsilon_\phi - n_x \sin\varepsilon_\phi, n_z)^{\mathrm{T}}$ captures an error pertaining to the direction of the rotation axis [45] whose original direction is specified by the unit vector $\hat{\mathbf{n}} \equiv (\cos\phi, \sin\phi, 0)^{\mathrm{T}}$.

In keeping with the above general considerations, it is pertinent to investigate the robustness of the W-to-GHZ state-conversion scheme based on the idealized

pulse sequence described in Sec. V A to systematic errors. Among them, it is worthwhile to consider errors in the rotation angles corresponding to the instantaneous control pulses (related to the parameters α_1 and α_2), errors pertaining to the directions of the attendant rotation axes (ϕ_1 and ϕ_2), as well as pulse-length errors of the Ising-interaction pulse (ξ). To this end, we consider errors of either sign for the five relevant parameters:

$$\begin{aligned} \xi &= \xi_0(1+\varepsilon_\xi)\,, \\ \alpha_j &= \alpha_{j,0}(1+\varepsilon_{\alpha_j})\,, \quad \phi_j = \phi_{j,0}+\varepsilon_{\phi_j} \quad (\,j=1,2\,)\,. \end{aligned} \tag{29}$$

Regarding the form of the last equation, it should be noted that the introduced errors in the parameters ξ, α_1, and α_2 have the character of relative errors, while for ϕ_1 and ϕ_2 it is more meaningful to consider absolute errors.

For general (i.e. not necessarily small) values of $\varepsilon_\xi, \varepsilon_{\alpha_1}, \varepsilon_{\phi_1}, \varepsilon_{\alpha_2}, \varepsilon_{\phi_2}$, the GHZ-state fidelity is given by

$$\begin{aligned} \mathcal{F}_{\rm GHZ}(\varphi,\varepsilon_\xi) &= \frac{1}{4}\left|3+e^{4i\xi_0\varepsilon_\xi}\right|, \\ \mathcal{F}_{\rm GHZ}(\varphi,\varepsilon_{\alpha_1}) &= \frac{1}{2}|\cos(\alpha_{1,0}\varepsilon_{\alpha_1})|\,|3\cos(2\alpha_{1,0}\varepsilon_{\alpha_1})-1|\,, \\ \mathcal{F}_{\rm GHZ}(\varphi,\varepsilon_{\phi_1}) &= \frac{1}{8}\left|3-2e^{i\varepsilon_{\phi_1}}+3e^{2i\varepsilon_{\phi_1}}\right|\left|1+e^{i\varepsilon_{\phi_1}}\right|, \\ \mathcal{F}_{\rm GHZ}(\varphi,\varepsilon_{\alpha_2}) &= \left|\cos(2\alpha_{2,0}\varepsilon_{\alpha_2})-\frac{i}{2}\,\sin(2\alpha_{2,0}\varepsilon_{\alpha_2})\right|, \\ \mathcal{F}_{\rm GHZ}(\varphi,\varepsilon_{\phi_2}) &= \frac{\sqrt{3}}{4}\left|\left(1+e^{6i\varepsilon_{\phi_2}}\right)c_-^3\right. \\ &\quad +i\left(e^{i\varepsilon_{\phi_2}}+e^{5i\varepsilon_{\phi_2}}\right)wc_+c_-^2 \\ &\quad +\left(e^{2i\varepsilon_{\phi_2}}+e^{4i\varepsilon_{\phi_2}}\right)wc_+^2c_- \\ &\quad \left.+2i\,e^{3i\varepsilon_{\phi_2}}c_+^3\right|\,, \end{aligned} \tag{30}$$

where w and $c_\pm$ stand for the following constants:

$$w=\frac{1+2\sqrt{2}i}{3} \quad , \quad c_\pm=\sqrt{\frac{\sqrt{3}\pm\sqrt{2}}{2\sqrt{3}}}\,. \tag{31}$$

It is interesting to note that none of the five expressions for $\mathcal{F}_{\rm GHZ}$ in Eq. (30) has any dependence on φ, even though the optimal values of the parameters ϕ_1 and ϕ_2 do depend on φ. This can be understood as a manifestation of the general notion that the most important global properties of GHZ-type states do not depend on φ [42].

We now turn our attention to the case of small deviations ($\varepsilon_p \ll 1$) from the optimal values of the relevant parameters ($p=\xi,\alpha_1,\phi_1,\alpha_2,\phi_2$). By expanding the respective expressions for the GHZ-state fidelity in Eq. (30) to the lowest nonvanishing (quadratic) order in ε_p, we obtain the following results:

$$\begin{aligned} \mathcal{F}_{\rm GHZ}(\varphi,\varepsilon_\xi) &= 1-\frac{3}{2}\,\xi_0^2\varepsilon_\xi^2+\mathcal{O}(\varepsilon_\xi^4)\,, \\ \mathcal{F}_{\rm GHZ}(\varphi,\varepsilon_{\alpha_1}) &= 1-\frac{7}{2}\,\alpha_{1,0}^2\varepsilon_{\alpha_1}^2+\mathcal{O}(\varepsilon_{\alpha_1}^4)\,, \\ \mathcal{F}_{\rm GHZ}(\varphi,\varepsilon_{\phi_1}) &= 1-\frac{7}{8}\,\varepsilon_{\phi_1}^2+\mathcal{O}(\varepsilon_{\phi_1}^4)\,, \\ \mathcal{F}_{\rm GHZ}(\varphi,\varepsilon_{\alpha_2}) &= 1-\frac{3}{2}\,\alpha_{2,0}^2\varepsilon_{\alpha_2}^2+\mathcal{O}(\varepsilon_{\alpha_2}^4)\,, \\ \mathcal{F}_{\rm GHZ}(\varphi,\varepsilon_{\phi_2}) &= 1-\left(2-\frac{3}{4}\sqrt{6}\right)\varepsilon_{\phi_2}^2+\mathcal{O}(\varepsilon_{\phi_2}^4)\,. \end{aligned} \tag{32}$$

Needless to say, the linear terms in these expansions vanish because the fidelity reaches its maximum for the considered values $\alpha_{1,0}=\pi/4$, $\phi_{1,0}=5\pi/6$, $\phi_{2,0}=\pi/3$, and $\xi_0=\alpha_{2,0}=\arccos(1/3)/4$ of the five relevant pulse-sequence parameters. Based on these values of the five relevant parameters [cf. Sec. V A], the prefactors of the quadratic terms in the expansions of Eq. (32) can straightforwardly be determined: $3\xi_0^2/2=0.142$, $7\alpha_{1,0}^2/2=2.159$, $7/8=0.875$, $3\alpha_{2,0}^2/2=0.142$, and $2-3\sqrt{6}/4=0.163$, respectively.

The small-ε_p expansions of $\mathcal{F}_{\rm GHZ}$ [cf. Eq. (32)], which quantify the relative impact on the target-state fidelity of the deviations ε_p in different parameters of relevance in the problem at hand, are illustrated in Fig. 3. What is evident from this figure is that – among the five relevant parameters – the GHZ-state fidelity is by far most sensitive to deviations in the value of α_1, i.e. the rotation angle corresponding to the first control pulse. Another salient feature of Eq. (32) is that the obtained expansions for α_2 and ξ are completely the same (cf. Sec. V A), with the results for ϕ_2 being just slightly different than those two (as can also be inferred from Fig. 3).

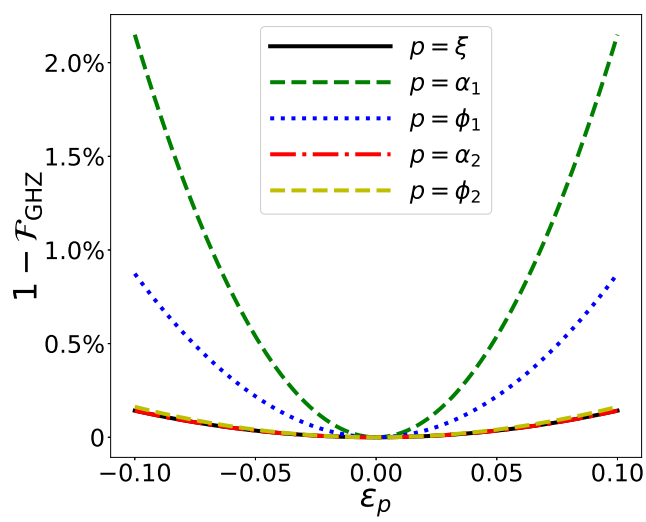

FIG. 3: (Color online)Deviation of the GHZ-state fidelity from unity (i.e. the infidelity) $1-\mathcal{F}_{\rm GHZ}$ as a function of errors ε_p in the values of the parameters that characterize the pulse sequence realizing the W-to-GHZ state conversion.

Another interesting conclusion can be drawn from the obtained prefactors to quadratic terms in ε_p in Eq. (32). Namely, the respective quantitative impacts on the fidelity $\mathcal{F}_{\rm GHZ}$ of errors in the parameters α_1 and α_2 (i.e. in the rotation angles corresponding to the $t = 0$ and $t = T$ control pulses) from their optimal values differ drastically, as can also be inferred from Fig. 3. More precisely, for the same error (i.e. for $\varepsilon_{\alpha_1} = \varepsilon_{\alpha_2} \equiv \varepsilon_\alpha$), the deviation in α_1 leads to an approximately 15 times larger reduction of the fidelity than that of α_2. Thus, our envisioned W-to-GHZ state-conversion scheme is much more sensitive to errors in the first control pulse (at $t = 0$) than those corresponding to the second one (at $t = T$). This last observation can be understood by analyzing the change in the target-state fidelity resulting from the first control pulse. Namely, this pulse leads to the change from $\mathcal{F}_{\rm GHZ} = 0$ to $\mathcal{F}_{\rm GHZ} = \sqrt{3}/2 \approx 0.866$, which implies that the first control pulse represents a much bigger stride towards the final GHZ state than the second one. This makes the numerical results presented in Fig. 3 – i.e. the much larger sensitivity of the state-conversion scheme at hand to errors in the first control pulse – completely plausible.

It is well-known that the entanglement-related properties of GHZ states are largely independent of the specific value of φ [cf. Eq. (6)]. For instance, GHZ states are characterized by maximal essential three-way entanglement, as quantified by the 3-tangle [76]), irrespective of the value of φ. Likewise, these states have no pairwise entanglement, as quantified by the vanishing pairwise concurrences [31]. Because of that, it makes sense to analyze the robustness of our envisaged pulse sequence to errors in situations where one does not prioritize obtaining a final GHZ state with the specific value of φ, but rather a GHZ state with an arbitrary φ. This last scenario alleviates the impact of the errors in the parameters ε_{ϕ_1} and ε_{ϕ_2} – whose optimal values depend on φ – on the GHZ-state fidelity in the following sense. Namely, if only the value of one angle – e.g., ϕ_1 – deviates from its optimal value $\phi_{1,0}$, the fidelity cannot reach unity for any φ since the found relationship between the optimal values of $\phi_{1,0}$ and $\phi_{2,0}$ – given by Eq. (25) – is not satisfied anymore. However, the final-state fidelity might increase and reach values very close to unity if φ is allowed to vary as well. In that case, we can de-facto treat φ as an additional variable parameter and try to optimize the final-state fidelity with respect to φ for the fixed value of the parameter ϕ_1 that deviates from its optimal value $\phi_{1,0}$. In other words, in the case of fixed φ the fidelity is computed for a specific, pre-determined value of φ and deviations from its corresponding optimal value of ϕ_1. By contrast, in the case that we do not prioritize obtaining a GHZ state with a specific value of φ – but, instead, any state of GHZ type – we choose for φ the value for which the final-state fidelity reaches its maximum, given the fixed value $\phi_{1,0} + \varepsilon_{\phi_1}$ of ϕ_1 (that deviates from $\phi_{1,0}$); this last maximum, in principle, need not be equal to unity. Both of these scenarios are illustrated in Fig. 4, where the relative impacts of the errors ε_{ϕ_1} and ε_{ϕ_2} on the fidelity $\mathcal{F}_{\rm GHZ}$ in the aforementioned cases of fixed- and arbitrary φ are compared. What is evident from this plot is that the deviation of the GHZ-state fidelity from unity due to deviations in ε_{ϕ_1} is drastically smaller in the latter case.

Aside from the expansions in Eq. (32), which quantify the impact of deviations ε_p in individual pulse-sequence parameters on the GHZ-state fidelity, it is pertinent to also discuss the effect of simultaneous errors in more than one parameter. To this end, the fidelity $\mathcal{F}_{\rm GHZ}$ is evaluated numerically based on its defining expression [cf. Eq. (21)], i.e. without resorting to the small-ε_p expansions in Eq. (32). For instance, Fig. 5 illustrates the deviation $1-\mathcal{F}_{\rm GHZ}$ of the fidelity from unity (the infidelity) for a range $[-0.1, 0.1]$ of values for simultaneous deviations in two different parameters. In particular, Fig. 5(a) illustrates the infidelity resulting from errors in the values of the parameters ϕ_1 and ϕ_2, while Fig. 5(b) shows the analogous dependence on errors in the parameters α_1 and α_2. In both cases, it is noticeable that even relatively large errors (such as 0.1) in these parameters result in a relatively small infidelity. As can be inferred from Fig. 5, the infidelity does not exceed 1.25% (2.5%) in the case of parameters ϕ_1 and ϕ_2 (α_1 and α_2).

Another situation worth discussing is the one involving simultaneous errors in the Ising-pulse duration ξ and the pair of parameters ϕ_1 and ϕ_2 (or α_1 and α_2). In particular, shown in Fig. 6(a) is the infidelity resulting from simultaneous errors in ξ, ϕ_1, and ϕ_2, where errors in the last two parameters are assumed to be the same (i.e. $\varepsilon_{\phi_1} = \varepsilon_{\phi_2} \equiv \varepsilon_\phi$). At the same time, Fig. 6(b) illustrates the infidelity resulting from errors in ξ, α_1, and α_2, where – by analogy with Fig. 6(a) – it was assumed that

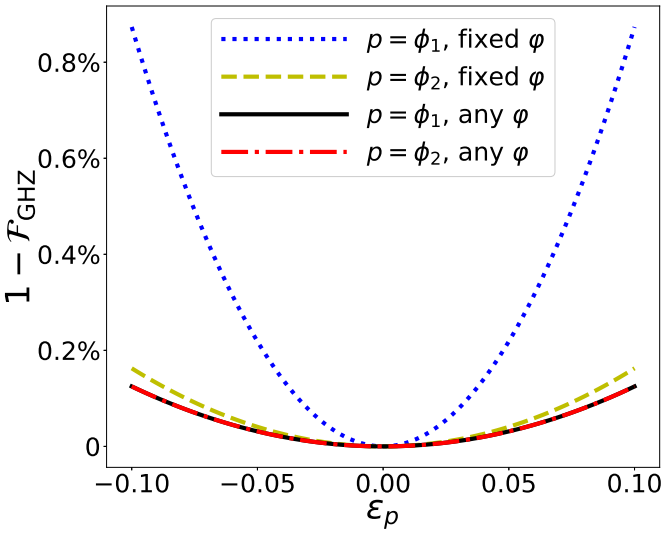

FIG. 4: (Color online)Comparison of the dependence of the infidelity $1 - \mathcal{F}_{\rm GHZ}$ on ε_{ϕ_1} and ε_{ϕ_2} for fixed- and arbitrary value of φ.

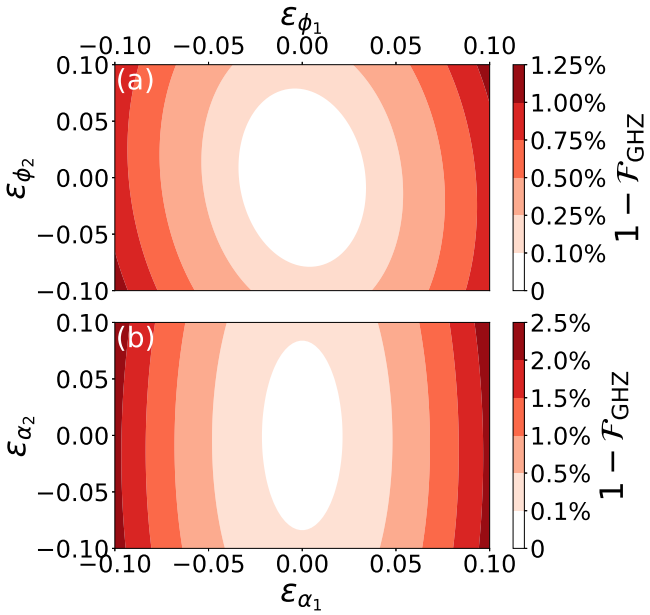

FIG. 5: (Color online)Deviation of the GHZ-state fidelity from unity (i.e. the infidelity) $1-\mathcal{F}_{\rm GHZ}$ as a function of (a) errors in the parameters ϕ_1 and ϕ_2, i.e. deviations from their respective optimal values $\phi_{1,0}=5\pi/6$ and $\phi_{2,0}=\pi/3$, and (b) errors in the parameters α_1 and α_2, i.e. deviations from their respective optimal values $\alpha_{1,0}=\pi/4$ and $\alpha_{2,0}=\arccos(1/3)/4$.

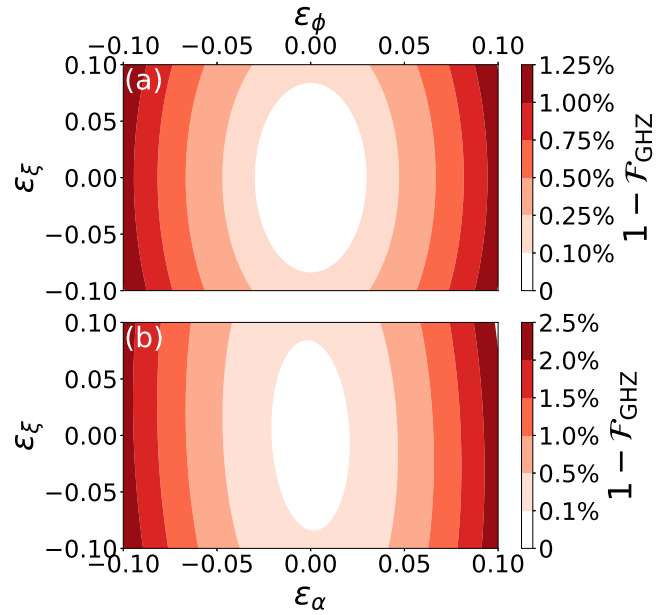

FIG. 6: (Color online)Deviation of the GHZ-state fidelity from unity (i.e. the infidelity) $1-\mathcal{F}_{\rm GHZ}$ as a function of (a) errors in the Ising-pulse duration ε_ξ and the angles $\varepsilon_{\phi_1}=\varepsilon_{\phi_2}\equiv\varepsilon_\phi$ specifying the two rotation axes, and (b) errors in ε_ξ and the two rotation-angles $\varepsilon_{\alpha_1}=\varepsilon_{\alpha_2}\equiv\varepsilon_\alpha$ corresponding to the instantaneous control pulses.

$\varepsilon_{\alpha_1}=\varepsilon_{\alpha_2}\equiv\varepsilon_\alpha$. What can be inferred from Fig. 6 is that even rather large deviations of the three relevant parameters – ξ, ϕ_1, ϕ_2 in Fig. 6(a) and ξ, α_1, α_2 in Fig. 6(b) – from their optimal values (up to $\varepsilon_p=0.1$) lead to relatively modest deviations of the GHZ-state fidelity from unity, which do not exceed 2.5%. This speaks in favor of the robustness of the envisioned W-to-GHZ state conversion to errors in the relevant parameters.

One common salient feature of Figs. 5 and 6 is the elliptical shape of their central, white-colored regions. This elliptical shape is a consequence of the fact that the lowest-order dependence of the GHZ-state fidelity on the error in the relevant parameters is quadratic. For instance, the lowest-order expansion of $1-\mathcal{F}_{\rm GHZ}$ in ε_ξ and ε_α [cf. Fig. 6(b)] is given by

$$1-\mathcal{F}_{\rm GHZ}(\varphi)=\frac{3}{2}\,\varepsilon_\xi^2+5\varepsilon_\alpha^2+\varepsilon_\xi\varepsilon_\alpha+\mathcal{O}\left[(\varepsilon_\alpha,\varepsilon_\xi)^3\right]\ , \quad (33)$$

which clearly describes an ellipse in the ε_ξ-ε_α plane. The other regions in Figs. 5 and 6 represent dilated versions of these central elliptically-shaped regions.

While here we have discussed in detail the robustness to errors of the pulse sequence for converting an initial W state into its GHZ counterpart, the robustness of the inverse (GHZ-to-W) state-conversion process can be analyzed in a completely analogous fashion.

VI. SUMMARY AND CONCLUSIONS

To summarize, in this paper we addressed the problem of interconversion between W and GHZ states for a three-qubit system with Ising-type coupling between qubits that are also subject to global transverse Zeeman-like control fields. Motivated in large part by a recent Lie-algebraic result that guarantees the state-to-state controllability of such a system for an arbitrary pair of initial and final states that are invariant with respect to permutations of qubits, we carried out our analysis within the four-dimensional subspace of the three-qubit Hilbert space that contains such (permutation-invariant) states.

We determined a solution of the W-to-GHZ state-conversion problem in the form of an NMR-type pulse sequence, which consists of two instantaneous (global) control pulses – each of them being equivalent to a global qubit rotation – and a finite-duration Ising-interaction pulse between them. We numerically obtained the optimal values of the five parameters (two rotation angles corresponding to the control pulses, two angles that define the directions of the corresponding rotation axes, and the duration of the Ising-interaction pulse) that describe the envisioned pulse sequence. We then demonstrated the robustness of the proposed pulse sequence to errors in its five characteristic parameters. In particular, we showed that the GHZ-state fidelity retains values very close to unity even for appreciable deviations of the relevant parameters from their optimal values.

Several generalizations of the present work can be envisaged. Firstly, the robustness of the proposed scheme to decoherence – an issue that necessitates treatment within the open-system scenario – is worthwhile investigating. Secondly, the same deterministic interconversion problem for W and GHZ states could also be studied for a system with more than three qubits; also, other state-interconversion problems – involving various types of generalized W and GHZ states, as well as other interesting classes of entangled states (e.g. Dicke-type states) – are also of appreciable interest. Finally, an analogous state-interconversion problem could be addressed for qubit arrays with other common types of qubit-qubit interactions, such as XY-type interactions of relevance for superconducting qubits [77] and Heisenberg-type interactions characteristic of spin qubits [58, 78].

Acknowledgments

The authors acknowledge useful discussions with G. Alber. This research was supported by the Deutsche Forschungsgemeinschaft (DFG) – SFB 1119 – 236615297.

[1] M. A. Nielsen and I. L. Chuang, *Quantum Computation and Quantum Information* (Cambridge University Press, Cambridge, 2000).
[2] M. A. Nielsen, Phys. Rev. Lett. **83**, 436 (1999).
[3] W. Dür, G. Vidal, and J. I. Cirac, Phys. Rev. A **62**, 062314 (2000).
[4] D. M. Greenberger, M. A. Horne, and A. Zeilinger, in *Bell's Theorem, Quantum Theory, and Conceptions of the Universe* (Kluwer Academic, Dordrecht, 1989), pp. 73-76.
[5] D. Zhu, G.-G. He, and F.-L. Zhang, Phys. Rev. A **105**, 062202 (2022).
[6] J. Joo, Y.-J. Park, S. Oh, and J. Kim, New J. Phys. **5**, 136 (2003).
[7] C. Zhu, F. Xu, and C. Pei, Sci. Rep. **5**, 17449 (2015).
[8] V. Lipinska, G. Murta, and S. Wehner, Phys. Rev. A **98**, 052320 (2018).
[9] W. K. C. Sun, A. Cooper, and P. Cappellaro, Phys. Rev. A **101**, 012319 (2020).
[10] S. Omkar, S.-H. Lee, Y. S. Teo, S.-W. Lee, and H. Jeong, PRX Quantum **3**, 030309 (2022).
[11] X. Peng, J. Zhang, J. Du, and D. Suter, Phys. Rev. Lett. **103**, 140501 (2009); Phys. Rev. A **81**, 042327 (2010).
[12] S. Dogra, K. Dorai, and Arvind, Phys. Rev. A **91**, 022312 (2014).
[13] C. Li and Z. Song, Phys. Rev. A **91**, 062104 (2015).
[14] Y.-H. Kang, Y.-H. Chen, Z.-C. Shi, J. Song, and Y. Xia, Phys. Rev. A **94**, 052311 (2016).
[15] Y.-H. Kang, Y.-H. Chen, Q.-C. Wu, B.-H. Huang, J. Song, and Y. Xia, Sci. Rep. **6**, 36737 (2016).
[16] B. Fang, M. Menotti, M. Liscidini, J. E. Sipe, and V. O. Lorenz, Phys. Rev. Lett. **123**, 070508 (2019).
[17] V. M. Stojanović, Phys. Rev. Lett. **124**, 190504 (2020).
[18] J. Peng, J. Zheng, J. Yu, P. Tang, G. A. Barrios, J. Zhong, E. Solano, F. Albarrán-Arriagada, and L. Lamata, Phys. Rev. Lett. **127**, 043604 (2021).
[19] V. M. Stojanović, Phys. Rev. A **103**, 022410 (2021).
[20] J. Zheng, J. Peng, P. Tang, F. Li, and N. Tan, Phys. Rev. A **105**, 062408 (2022).
[21] G.-Q. Zhang, W. Feng, W. Xiong, Q.-P. Su, and C.-P. Yang, arXiv:2205.13920.
[22] A. S. Coelho, F. A. S. Barbosa, K. N. Cassemiro, A. S. Villar, M. Martinelli, and P. Nussenzveig, Science **326**, 823 (2009).
[23] X. Wang, A. Bayat, S. G. Schirmer, and S. Bose, Phys. Rev. A **81**, 032312 (2010).
[24] C. Song, K. Xu, W. Liu, C.-P. Yang, S.-B. Zheng, H. Deng, Q. Xie, K. Huang, Q. Guo, L. Zhang, *et al.*, Phys. Rev. Lett. **119**, 180511 (2017).
[25] M. Erhard, M. Malik, M. Krenn, and A. Zeilinger, Nat. Photon. **12**, 759 (2018).
[26] V. Macrì, F. Nori, and A. Frisk Kockum, Phys. Rev. A **98**, 062327 (2018).
[27] R.-H. Zheng, Y.-H. Kang, Z.-C. Shi, and Y. Xia, Ann. Phys. (Berlin) **531**, 1800447 (2019).
[28] E. Pachniak and S. A. Malinovskaya, Sci. Rep. **11**, 12980 (2021).
[29] J. Nogueira, P. A. Oliveira, F. M. Souza, and L. Sanz, Phys. Rev. A **103**, 032438 (2021).
[30] Y.-F. Qiao, J.-Q. Chen, X.-L. Dong, B.-L. Wang, X.-L. Hei, C.-P. Shen, Y. Zhou, and P.-B. Li, Phys. Rev. A **105**, 032415 (2022).
[31] R. Horodecki, P. Horodecki, M. Horodecki, and K. Horodecki, Rev. Mod. Phys. **81**, 865 (2009).
[32] P. Walther, K. J. Resch, and A. Zeilinger, Phys. Rev. Lett. **94**, 240501 (2005).
[33] W. X. Cui, S. Hu, H. F. Wang, A. D. Zhu, and S. Zhang, Opt. Express **24**, 15319 (2016).
[34] Y. H. Kang, Z. C. Shi, B. H. Huang, J. Song, and Y. Xia, Phys. Rev. A **100**, 012332 (2019).
[35] J. Song, X. D. Sun, Q. X. Mu, L. L. Zhang, Y. Xia, and H. S. Song, Phys. Rev. A **88**, 024305 (2013).
[36] G. Y. Wang, D. Y. Wang, W. X. Cui, H. F. Wang, A. D. Zhu, and S. Zhang, J. Phys. B **49**, 065501 (2016).
[37] For an extensive review, see, e.g., M. Morgado and S. Whitlock, AVS Quantum Sci. **3**, 023501 (2021).
[38] For an up-to-date review, see X.-F. Shi, Quantum Sci. Technol. **7**, 023002 (2022).
[39] R.-H. Zheng, Y.-H. Kang, D. Ran, Z.-C. Shi, and Y. Xia, Phys. Rev. A **101**, 012345 (2020).
[40] T. Haase, G. Alber, and V. M. Stojanović, Phys. Rev. A **103**, 032427 (2021).
[41] T. Haase, G. Alber, and V. M. Stojanović, Phys. Rev. Research **4**, 033087 (2022).
[42] J. K. Nauth and V. M. Stojanović, Phys. Rev. A **106**, 032605 (2022).
[43] J. A. Jones, Phys. Rev. A **67**, 012317 (2003).
[44] C. Jones, M. A. Fogarty, A. Morello, M. F. Gyure, A. S. Dzurak, and T. D. Ladd, Phys. Rev. X **8**, 021058 (2018).
[45] For a review, see L. M. K. Vandersypen and I. L. Chuang, Rev. Mod. Phys. **76**, 1037 (2005).
[46] L. Viola, E.M. Fortunato, M.A. Pravia, E. Knill, R.

Laflamme, and D.G. Cory, Science **293**, 2059 (2001).
[47] E. M. Fortunato, L. Viola, M. A. Pravia, E. Knill, R. Laflamme, T. F. Havel, and D. G. Cory, Phys. Rev. A **67**, 062303 (2003).
[48] F. Albertini and D. D'Alessandro, J. Math. Phys. **59**, 052102 (2018).
[49] C. D. Hill, Phys. Rev. Lett. **98**, 180501 (2007).
[50] M. R. Geller, E. J. Pritchett, A. Galiautdinov, and J. M. Martinis, Phys. Rev. A **81**, 012320 (2009).
[51] J. Ghosh and M. R. Geller, Phys. Rev. A **81**, 052340 (2010).
[52] See, e.g, T. Tanamoto, Phys. Rev. A **88**, 062334 (2013).
[53] R. Raussendorf and H. J. Briegel, Phys. Rev. Lett. **86**, 5188 (2001).
[54] T. Tanamoto, D. Becker, V. M. Stojanović, and C. Bruder, Phys. Rev. A **86**, 032327 (2012).
[55] T. Tanamoto, V. M. Stojanović, C. Bruder, and D. Becker, Phys. Rev. A **87**, 052305 (2013).
[56] D. D'Alessandro, *Introduction to Quantum Control and Dynamics* (Taylor & Francis, Boca Raton, 2008).
[57] X. Wang, D. Burgarth, and S. G. Schirmer, Phys. Rev. A **94**, 052319 (2016).
[58] R. Heule, C. Bruder, D. Burgarth, and V. M. Stojanović, Phys. Rev. A **82**, 052333 (2010); Eur. Phys. J. D **63**, 41 (2011).
[59] J. Zhang and K. B. Whaley, Phys. Rev. A **71**, 052317 (2005).
[60] P. Zanardi, Phys. Rev. A **60**, R729 (1999).
[61] P. Ribeiro and M. Mosseri, Phys. Rev. Lett. **106**, 180502 (2011).
[62] A. Burchardt, J. Czartowski, and K. Życzkowski, Phys. Rev. A **104**, 032442 (2021).
[63] C. Chryssomalakos, L. Hanotel, E. Guzmán-González, D. Braun, E. Serrano-Ensástiga, and K. Życzkowski, Phys. Rev. A **104**, 032442 (2021).
[64] M. Hebenstreit, C. Spee, N. Kai Hong Li, B. Kraus, and J. I. de Vicente, Phys. Rev. A **105**, 032458 (2022).
[65] D. W. Lyons, J. R. Arnold, and A. F. Swogger, Phys. Rev. A **105**, 032442 (2022).
[66] J. S. Kim, Sci. Rep. **8**, 12245 (2018).
[67] A. Acín, A. Andrianov, L. Costa, E. Jané, J. I. Latorre, and R. Tarrach, Phys. Rev. Lett. **85**, 1560 (2000).
[68] T. Xia, M. Lichtman, K. Maller, A. W. Carr, M. J. Piotrowicz, L. Isenhower, and M. Saffman, Phys. Rev. Lett. **114**, 100503 (2015).
[69] D. C. McKay, C. J. Wood, S. Sheldon, J. M. Chow, and J. M. Gambetta, Phys. Rev. A **96**, 022330 (2017).
[70] S. Debnath, N. M. Linke, C. Figgatt, K. A. Landsman, K. Wright, and C. Monroe, Nature (London) **536**, 63 (2016).
[71] T. M. Graham, M. Kwon, B. Grinkemeyer, Z. Marra, X. Jiang, M. T. Lichtman, Y. Sun, M. Ebert, and M. Saffman, Phys. Rev. Lett. **123**, 230501 (2019).
[72] See, e.g., Quantinuum, System Model H1 Product Data Sheet, Version 5.00 (2022).
[73] T. Ichikawa, U. Güngördü, M. Bando, Y. Kondo, and M. Nakahara, Phys. Rev. A **87**, 022323 (2013).
[74] E. Farhi, J. Goldstone, and S. Gutmann, arXiv:1411.4028 (2014).
[75] The reference material is given at the following URL: https://docs.scipy.org/doc/scipy/reference/generated/scipy.optimize.minimize.html.
[76] V. Coffman, J. Kundu, and W. K. Wootters, Phys. Rev. A **61**, 052306 (2000).
[77] V. M. Stojanović, A. Fedorov, A. Wallraff, and C. Bruder, Phys. Rev. B **85**, 054504 (2012).
[78] See, e.g., V. M. Stojanović, Phys. Rev. A **99**, 012345 (2019).